ALPHABETICAL INDEX BY AUTHOR'S NAME

Journal of Marine Research, 63, 1001–1015, 2005

Journal of MARINE RESEARCH

Volume 63, Number 6

Interfacial solitary wave run-up in the St. Lawrence Estuary

by Daniel Bourgault[1], Daniel E. Kelley[2] and Peter S. Galbraith[3]

ABSTRACT

Density variations show evidence of interfacial solitary waves (ISW) running up the sloping boundary of an island in the St. Lawrence Estuary, confirming inferences based remote sensing. Further detail is suggested by simulations created with a two-dimensional nonhydrostatic numerical model. The simulations confirm theoretical predictions of the location of wave breaking, something that is difficult to observe in the field. Two other results of the simulations match laboratory findings: the creation of turbulent boluses that propagate upslope of the breaking zone, and the creation of an intermediate layer that transports mixed water away from the mixing site. Although our sampling could not resolve the intermediate mixing layer, it did provide evidence of boluses. In addition to ISW breaking the bolus and intrusion effects may also be important in coastal regions.

1. Introduction

Tidally-driven interfacial solitary waves (ISW) were observed to collide against the lateral boundaries of the St. Lawrence Estuary by Bourgault and Kelley (2003), using shorebased photography. The results of that study suggested that the vertical mixing induced by ISW breaking on the slope, although sporadic and localized to the swash zone, may yield tidally- and laterally-averaged mixing rates that are comparable to shear-induced rates in a three-dimensional tidal circulation model of the estuary (Saucier and Chassé, 2000).

Unfortunately, there are no available direct field measurements of ISW-induced bound-

1. Department of Physics and Physical Oceanography, Memorial University of Newfoundland, St. John's, NL, Canada, A1B 3X7. ***email: danielb@physics.mun.ca***

2. Department of Oceanography, Dalhousie University, Halifax, NS, Canada, B3H 4J1.

3. Division of Ocean Sciences, Maurice Lamontagne Institute, Department of Fisheries and Oceans, Mont-Joli, QC, Canada, G5H 3ZA.

ary mixing in this estuary to verify the Bourgault and Kelley (2003) hypothesis. The collection of such field measurements in context requires an imposing experimental procedure, given the need to understand the processes of ISW generation, propagation, and interaction with boundaries.

As a first step toward the general goal of quantifying boundary mixing, and to help in coordinating future field investigations, we undertook an exploratory field experiment in the region identified by Bourgault and Kelley (2003) as a site of ISW run-up. We discuss these observations here, along with the results of numerical simulations done to aid in their interpretation. In providing field evidence of a process often idealized in the laboratory (Helfrich, 1992; Michallet and Ivey, 1999) and in models (Vlasenko and Hutter, 2002), we hope to contribute to the understanding of interfacial solitary waves in the coastal environment.

2. Geographical context

Figure 1 shows the study area in the St. Lawrence Estuary. Recent reviews of the general oceanography of the estuary are given by Saucier and Chassé (2000) and Bourgault and Kelley (2003). Only a summary on ISW boundary mixing is provided here.

The thick curve on Figure 1 depicts the position, observed by Bourgault and Kelley (2003), of the leading wave of a tidally-driven large-amplitude ISW packet that appears around three hours after the time of low water (LW + 3.00)[4]. The echo-sounder traces from another field season (Bourgault *et al.,* 2001) reveal that the ISWs have amplitude $a_0 \sim 15$ m; compared to the surface layer thickness $h_1 \sim 10$ m this indicates a nonlinear character of the ISWs.

This wavetrain heads toward the nearly uniform shoaling edge of Ile-aux-Lièvres where it is suspected to break around the 30 m isobath (Bourgault and Kelley, 2003) and thus enhance mixing shoreward of the breaking depth. The wave-island collision occurs at an angle of roughly 45° in the southern part of the island, while the collision is close to being orthogonal in the northern part.

Combining these observations with numerical simulations and results from the laboratory experiment of Michallet and Ivey (1999) for ISW running orthogonally into linear slopes, Bourgault and Kelley (2003) attempted to determine the wave energy budget. They concluded that the wavetrain carries roughly 4 MJ m^{-1} (energy per unit distance along the wave crest) to the island slope. Assuming that the laboratory findings of Michallet and Ivey (1999) on ISW energy transfer apply to the estuary, Bourgault and Kelley (2003) inferred that the tidally- and laterally-averaged ISW-induced vertical buoyancy flux for the region to be roughly $\bar{J} = 6 \times 10^{-4}$ W m^{-2}.

The results of this prior work, based on remote sensing observations and indirect

4. For ease of comparison with the Atlas of Tidal Currents (Government of Canada, 1997), the time in the text and figures is expressed as the number of hours relative to the time of low-water (LW, henceforth) at the Pointe-au-Père tidal gauge, the location of which is indicated in the inset of Figure 1.

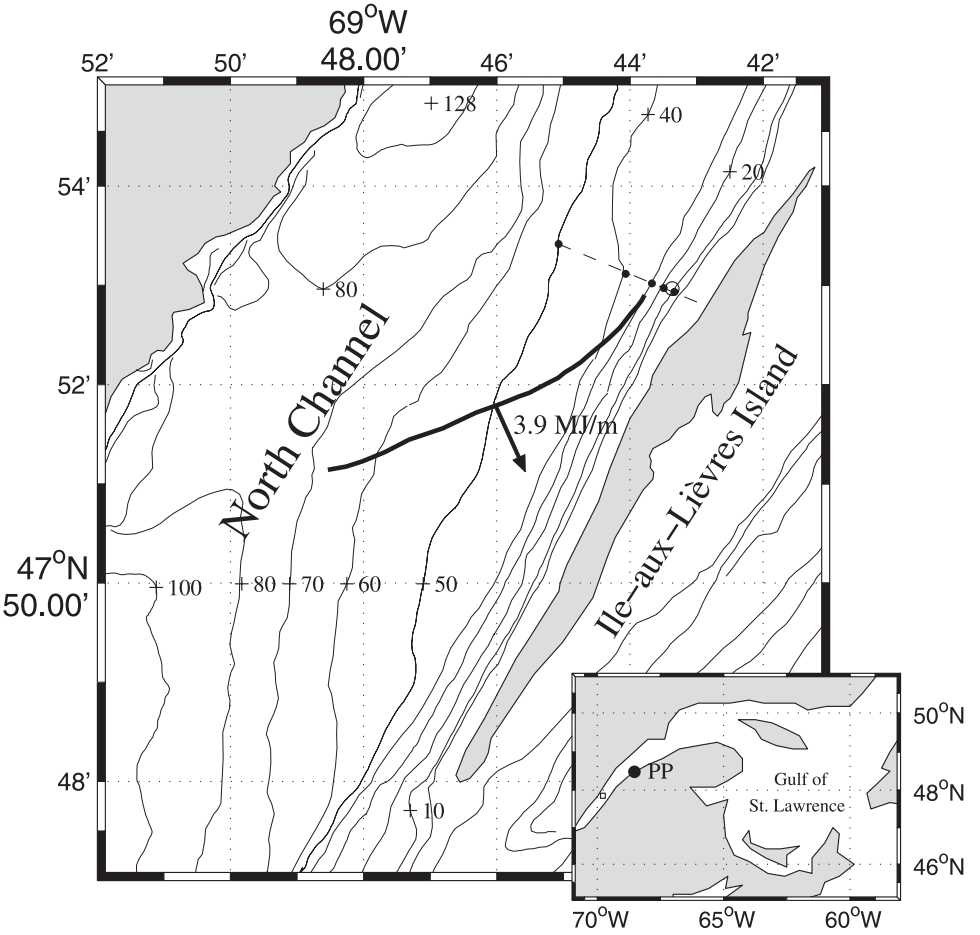

Figure 1. Map of the study region in the St. Lawrence Estuary. The position of the internal wavetrain crest observed by Bourgault and Kelley (2003) at LW + 3.00 in August 2000 is indicated, along with its propagation direction and energy of 3.9 MJ m^{-1}. The dashed line near the north end of the island indicates a cross-slope transect sampled in the present study, with dots representing CTD stations and the open circle indicating the CTD-chain anchor station. The inset illustrates the location of the Pointe-au-Père tidal gauge, marked PP, which provides the low-water time reference used in the text.

calculations, motivated the present study to look for ISWs near Ile-aux-Lièvres using *in situ* measurements, as described in the next section.

3. Methods

a. Field study

The sampling was carried out in August 2002 with a 10 m vessel. Given the Bourgault and Kelley (2003) results of the phase-locking of the ISW packets to the tide, the sampling

was keyed to the tidal phase. The field work involved both conductivity-temperature-depth profiler (CTD) transects and CTD-chain anchor stations.

The first step was to carry out CTD profiles at 5 stations along a transect orthogonal to the island edge (solid circles on Fig. 1). This section was selected because Bourgault and Kelley (2003) found that ISWs collide at almost right angles to the isobaths there. The new measurements were made just before the expected time of ISW impact, with the aim of measuring the stratification to be experienced by the ISWs as they collided with the sloping bottom.

At the end of the transect, the boat was taken to a location along the 20 m isobath (open circle on Fig. 1) to do an anchor station covering the expected time of ISW collision with the slope. This station was located in the predicted ISW surf and swash zone, slightly inshore of the predicted breaking depth ($H_b = 30$ m, according to Bourgault and Kelley (2003); see more below). The sampling involved the use of either two or three CTD sensors attached at different depths along a line. This CTD chain sampled between 0.5 Hz and 2 Hz for approximately 4 hours around the time where ISWs were most expected to occur, i.e. between LW + 2.00 and LW + 6.00. Since the CTD packages were not anchored to the bottom, and since the currents are large, the CTDs moved vertically throughout the time series as discussed in Section 4. The CTD transect was repeated at the completion of the anchor sampling station.

The initial plan was to collect measurements during the flooding phase of every second tidal cycle between August 23 and August 30, 2002. However, rough weather and technical difficulties limited the sampling to 3 cycles, on August 23, 27 and 28. Figure 2 shows the sampling periods relative to the tidal phase.

b. Numerical model

Recognizing that the field program had relatively sparse sampling, we set up a numerical model to help us interpret the measurements and to provide insights into the temporal and spatial scales that we were not able to measure. Three-dimensional nonhydrostatic models are too computationally expensive for this application, so we used a two-dimensional approach. The model was described by Bourgault and Kelley (2004) to which the reader is referred for details and validation.

We set up the model with the hydrography for application to ISW running into Ile-aux-Lièvres. The bathymetry was taken from the transect where CTD measurements were made (Fig. 1). The horizontal and vertical resolution grid spacing were $\Delta x = 1$ m and $\Delta z = 0.25$ m, respectively. A frictional bottom boundary condition was used with the roughness length set to $l_0 = 1.5 \times 10^{-4}$ m (see Bourgault and Kelley (2004) for details).

The initial background density was set to

$$\sigma_t(x, z) = \sigma_0 + \frac{\Delta\sigma}{2}\left[1 + \tanh\left(\frac{z - z_0}{\delta}\right)\right], \tag{1}$$

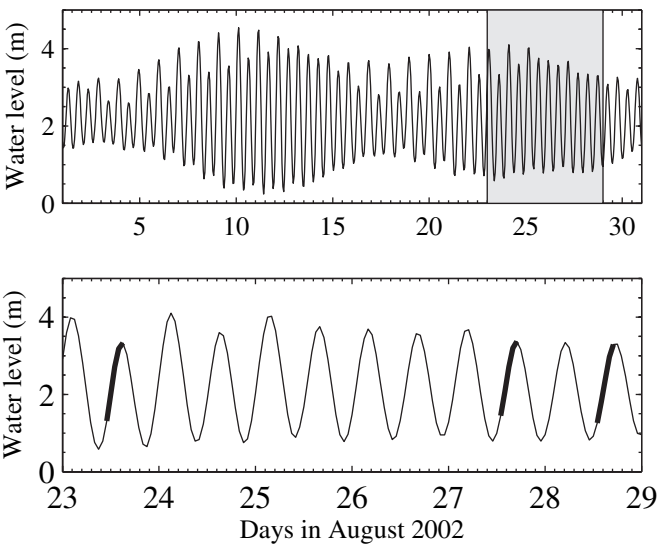

Figure 2. Water level during August 2002 at the Pointe-au-Père tidal gauge (see Fig. 1). The upper panel provides the spring-neap context, and the thick traces on the lower panel indicate the sampling times.

with z positive downward. Motivated by the observations (next section) we examined limiting cases of lower and higher stratification. For the low stratification case we set σ_0, $\Delta\sigma$, z_0, and δ to 19.5 kg m^{-3}, 4.5 kg m^{-3}, 10 m, and 3.5 m, respectively. For the high-stratification case, the corresponding values were 18.5 kg m^{-3}, 5.5 kg m^{-3}, 10 m, and 2 m (see Fig. 4). Figure 3 shows the model geometry and the initial density field (low stratification case) used to generate a shoreward propagating ISW of amplitude $a_0 = 15$ m breaking on Ile-aux-Lièvres.

4. Results

a. Field results

i. Profiles and transects. Figure 4 shows profiles of density σ_t and squared buoyancy frequency N^2 observed in the estuary interior (i.e. deepest station) before the expected occurrence of ISWs. From August 23 to August 28, the depth of the pycnocline varied from 8 m to 13 m, the stratification at the pycnocline varied from $N^2 = 12 \times 10^{-3}$ s^{-2} to $N^2 = 6 \times 10^{-3}$ s^{-2} and the density difference between bottom and surface varied from $\Delta\sigma =$ 5.5 kg m^{-3} to $\Delta\sigma = 4.5$ kg m^{-3}. On August 23 the density exhibits a two-layer structure while on August 27 and 28 a three-layer structure is observed with stratification in the top 5 m reaching $N^2 = 8 \times 10^{-3}$ s^{-2}.

Figure 5 shows the cross-sectional density field collected at LW + 6.5 on August 28. The stratification in the estuary interior extends to the boundary region, thus providing a

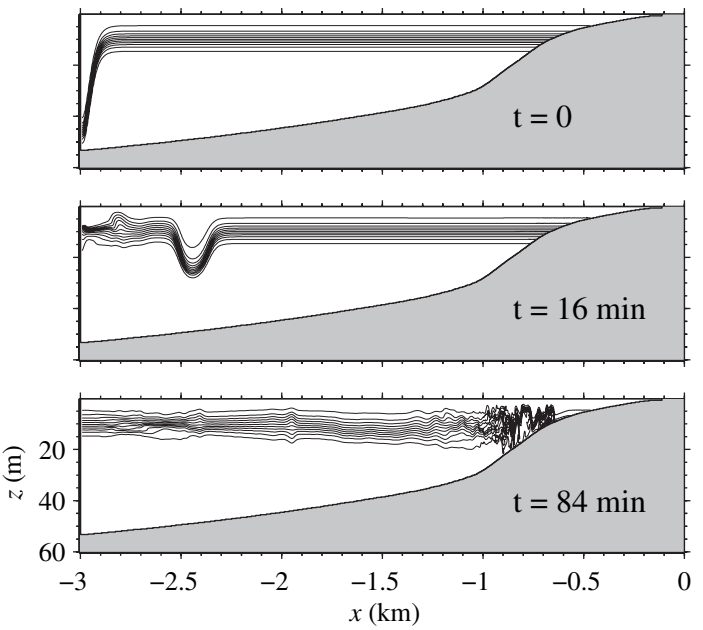

Figure 3. Model geometry and initial density field (top) used to generate a large amplitude solitary wave (middle) breaking and running into the shoaling slope of Ile-aux-Lièvres (bottom).

waveguide for ISWs to reach the pycnocline-bottom intersection. Other transects collected on August 23 and 27 did not reveal important variation from this general cross-sectional density structure and are omitted for conciseness.

The observations of Figure 5 also reveal the existence of a cross-channel density gradient below 20 m of $\partial\rho/\partial x = -4 \times 10^{-4}$ kg m^{-4}. Since this is of the same order of magnitude as the along-channel estuarine density gradient $\partial\rho/\partial y \sim 10^{-4}$ kg m^{-4} (e.g. Pelletier and Lebel, 1979), one might anticipate that this will yield a circulation of the same order of magnitude as the along-channel estuarine circulation. This hypothesis is yet to be tested in the field.

ii. Fixed station. Figure 6 shows time series of the densities of the suspended CTDs, and the depths recorded by each. (Recall that the CTDs were deployed along an unanchored line that tilted in the current.)

The depth measurements indicate that the CTDs remained at relatively fixed depths from LW + 2.00 to LW + 4.00 but that they shallowed by about 5 m from LW + 4.00 to LW + 6.00. This is presumably a result of increasing tidal currents, which reach 2.5 m s^{-1} at this phase of the tide (Saucier and Chassé, 2000). Out of a desire to study ISW dynamics in isolation of strong background current, we henceforth focus on the earlier time interval, LW + 2.00 to LW + 4.00, despite the existence of interesting signals throughout the sampling period.

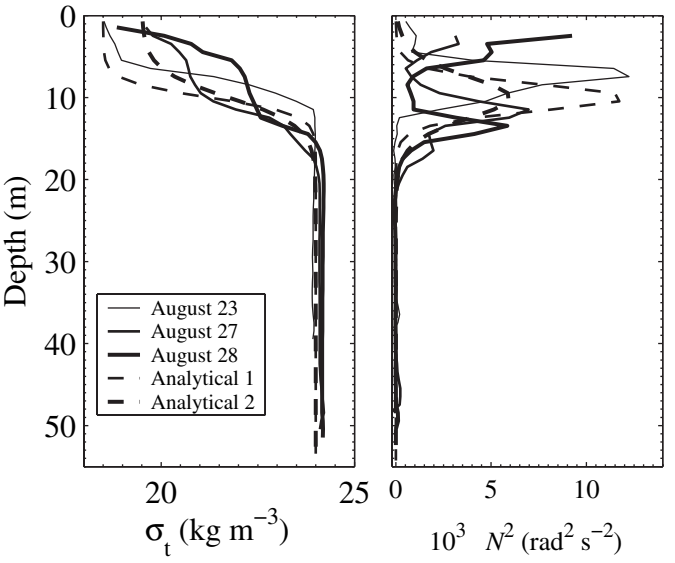

Figure 4. Density and squared buoyancy frequency in the estuary interior before the expected occurrences of ISW (i.e. before LW + 2.00). Also shown are two analytical profiles used to represent high and low stratification in the numerical simulations.

As anticipated from the Bourgault and Kelley (2003) study, frequent variations were recorded in the density time series. These variations, which reached 5 kg m^{-3}, were mainly observed below the mean pycnocline (i.e. below ~10 m). An exception is the period from

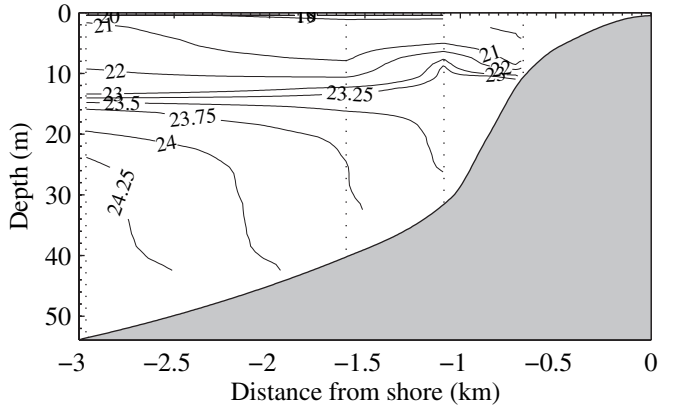

Figure 5. Cross section of the density σ_t field measured at LW + 6.5 on August 28. The vertical dotted lines represent the density profiles from which the field was interpolated (i.e. stations identified by the solid circles on Fig. 1).

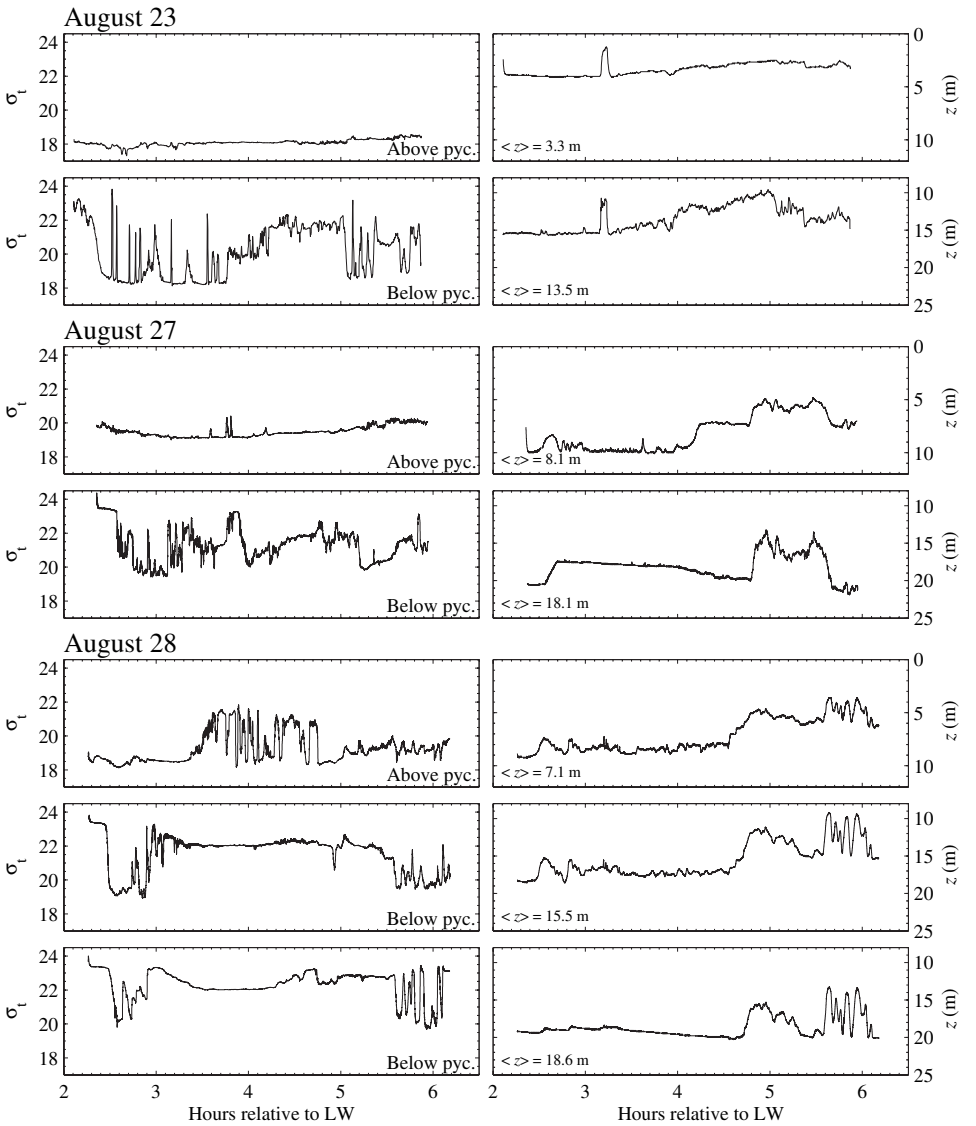

Figure 6. Time series of density (left panels) and depth of the CTDs (right panels) recorded at the anchored site. The "above/below pyc." notation indicates whether the CTD was located above or below the pycnocline. The $\langle z \rangle$ notation indicates the average depth of the CTDs.

LW + 3.50 to LW + 5.00 on August 28, during which high frequency fluctuations were recorded above the pycnocline but not below it.

The variation in the earlier part (i.e. from LW + 2.0 to LW + 3.0) of all three time series exhibits a repetitive pattern. There is an initial drop in density by around 4 kg m^{-3}, which

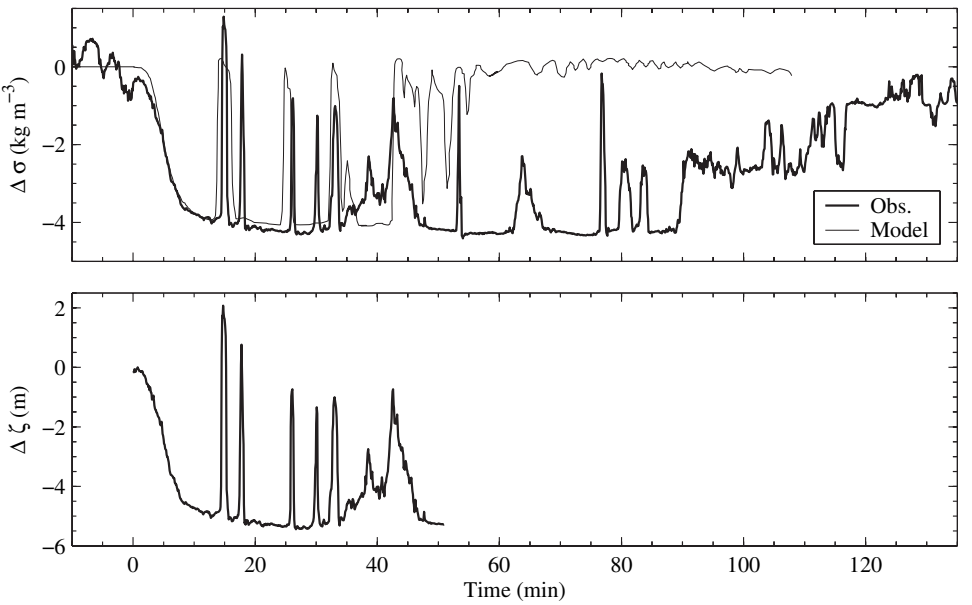

Figure 7. Top: Comparison between recorded (thick line) and simulated (thin line) density fluctuations $\Delta\sigma$ at $z = 15$ m where the total depth is 20 m (i.e. at $x = -850$ m in the simulation). For comparison with the numerical simulations the time in this figure is relative to the timing of the initial density drop. Bottom: Vertical displacements as calculated by (2).

takes place over a 5 min interval at around LW + 2.4, after which follow distinct rises in density as well as other irregular fluctuations. This pattern is most noticeable on August 23 and is shown in greater detail in Figure 7. These individual rising events have duration that varies from 60 s (e.g. the event around 18 min) to 300 s (e.g. the event around 64 min). Thus, the shortest of these events has a duration comparable to the buoyancy period of roughly 60 s.

To help interpret these observations we reproduce in Figure 8 the laboratory observations of Helfrich (1992) for an experiment on ISW breaking and run-up on a uniform slope. These display a similar pattern to the field measurements, with an initial, slow reduction in density being followed by a sequence of isolated bursts of increased density. The similarity between the laboratory observations and the field results suggests that similar phenomena occur in each case. The laboratory shadowgraphs showed that these events are generated during the breaking, and subsequent running-up, of ISWs on sloping boundaries. These events were named "turbulent boluses" by Helfrich (1992) and so we will designate them as such henceforth. We thus interpret our observations as evidence of ISW breaking on the slope of Ile-aux-Lièvres.

A time series of the isopycnal displacement $\Delta\zeta(t)$ was estimated by

$$\Delta\zeta = \Delta\sigma\left(\frac{d\hat{\sigma}}{dz}\right)^{-1}, \tag{2}$$

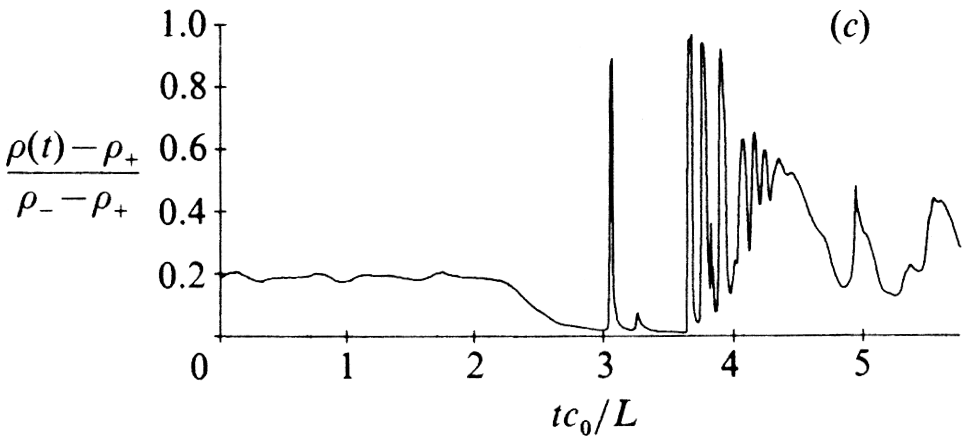

Figure 8. Reproduction of the Helfrich (1992) figure illustrating laboratory measurements of density time series at the interface-slope intersection in an experiment with two incident solitary waves running into a shoaling linear slope. The abscissa is nondimensional time and the ordinate is nondimensional density.

where $\Delta\sigma$ is the difference between the instantaneous density and the density taken just before the arrival of the wave, and $d\hat{\sigma}/dz$ is a time-invariant background density gradient calculated from nearby hydrographic surveys. This gradient was derived from a least-squared linear model of the form $z = z(\hat{\sigma})$, using only measurements in the 5 m to 17 m depth range of the mooring. To avoid confounding effects of instrument movement, (2) was applied only to intervals during which the instruments moved no more than 1 m vertically. For example, for the August 23 data this condition was met by the period from LW + 2.00 to LW + 3.00. According to this procedure, the boluses observed have maximum vertical displacement 5 m $\leq |\Delta\zeta|_{\max} \leq$ 7 m (Fig. 7).

b. Model results

i. Description of wave breaking. Figure 9 shows the simulated evolution of the density field upon the impact of an ISW with the sloping boundary of Ile-aux-Lièvres. The results for the case of a wavetrain collision are qualitatively similar. The simulation shows the laminar incoming ISW evolving into a complex turbulent field upon collision with the shoaling bottom. Many spiral features, typical of shear instabilities, and other more complex density overturning structures are generated as the wave breaks and runs up the slope. The largest of these overturns (e.g. the series of three billows seen around $x = -0.9$ km at $t = 10$ min in Fig. 9) have vertical and horizontal scales of 10 m and 20 m, respectively.

The transition from laminar to turbulent flow occurs at the wave breaking depth $H_b =$ 29 m, determined as the depth at the location of the first occurrence of a density

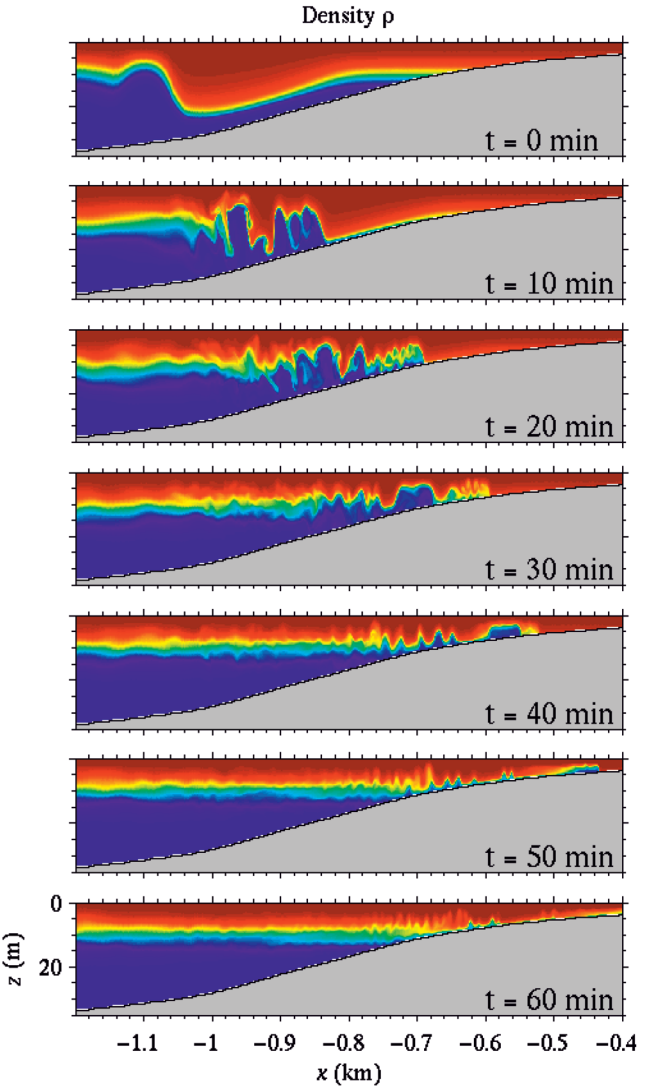

Figure 9. Simulated evolution of the density field upon impact of a single solitary wave with the sloping boundary of Ile-aux-Lièvres.

overturning event. This value for the breaking depth derived from the numerical model can be compared to the Vlasenko and Hutter (2002) breaking criterion for linear slopes,

$$H_b = h_1 + a_0 \frac{\theta}{0.8^\circ + 0.4\theta}, \tag{3}$$

in which θ is the uniform bottom slope (in degrees above horizontal), a_0 is the wave amplitude and h_1 is the surface layer thickness. Because the slope of Ile-aux-Lièvres is

nonuniform, there is some ambiguity regarding the choice of θ in applying (3) to this environment. For example, the steepest slope, between $-0.9 \leq x \leq -0.8$ km, is $\theta = 3.3°$ while at the pycnocline-bottom intersection, i.e. at $x = -0.65$ km, $\theta = 1.9°$. Given this range of uncertainty for θ, and using $a_0 = 15$ m and $h_1 = 10$ m we obtain $28 \leq H_b \leq 33$ m. The modeled breaking depth is thus consistent to the Vlasenko and Hutter (2002) formulation to within the uncertainty.

ii. Onshore-propagating boluses. Isolated features reminiscent of up-slope propagating turbulent boluses observed in the laboratory are also seen in the numerical simulations. These are most noticeable for $t \geq 40$ min in Figure 9. Some of these boluses exhibit the shape of internal solitary waves of elevation that are characterized with typical wavelength of 10 m and amplitude of 5 m (e.g. at around $x = -0.65$ km at $t = 40$ min). Other bolus-like features exhibit more irregular shapes such as the 40 m long and 4 m thick structure seen around $x = -0.6$ km at $t = 40$ min. These modeled bolus amplitudes are comparable to the vertical displacements inferred from the CTD measurements in Section 4a(ii), supporting the idea that we have observed ISW run-up in our field study.

A simulation of the density time series that an instrument would measure at $z = 15$ m in a total depth of 20 m is shown in Figure 7 and compared to the field measurements of August 23. The simulated time series shares many characteristics with the field observations as well as with the laboratory results of Helfrich (1992) as reproduced in our Figure 8. Prominently, it shows a roughly 5 min duration decrease in density as the wave approaches the instrument, after which there are several abrupt density increases, each lasting of order 2 minutes. Thus, the timescales also suggest we have observed boluses generated by ISWs running-up Ile-aux-Lièvres.

A potentially important aspect of the boluses revealed by the numerical simulations is their role in transporting sub-pycnocline water up-slope past the pycnocline-bottom intersection. Boluses transporting sub-pycnocline water, i.e. water found below 10 m in the undisturbed state (coded blue in Fig. 9), are evident as far inshore as the 5 m isobath. An estimation of the volume of sub-pycnocline water transported by these boluses can be made by estimating the area of the boluses found above the pycnocline. For example, the bolus at $t = 40$ min and $x = -0.6$ km is roughly 40 m long and 4 m thick. This bolus thus transports 160 m^3 per unit meter of island length, of sub-pycnocline water up-slope. This wave-induced advective flux may be important for bringing into the surface layer nutrient-rich sub-pycnocline water and may thus impact the local marine ecosystem. It is worth noting that the region around Ile-aux-Lièvres is recognized to be strategically important for the marine ecosystem of the St. Lawrence Estuary (especially for marine mammals and birds) (Bédard *et al.,* 1997).

iii. Offshore-propagating intrusive layer. To investigate the fate of water in the bottom homogeneous layer, an artificial pseudo-tracer was inserted. The initial tracer concentration field C was defined to be a linear function of the depth z,

$$C(x, z, t = 0) = z/z_0, \tag{4}$$

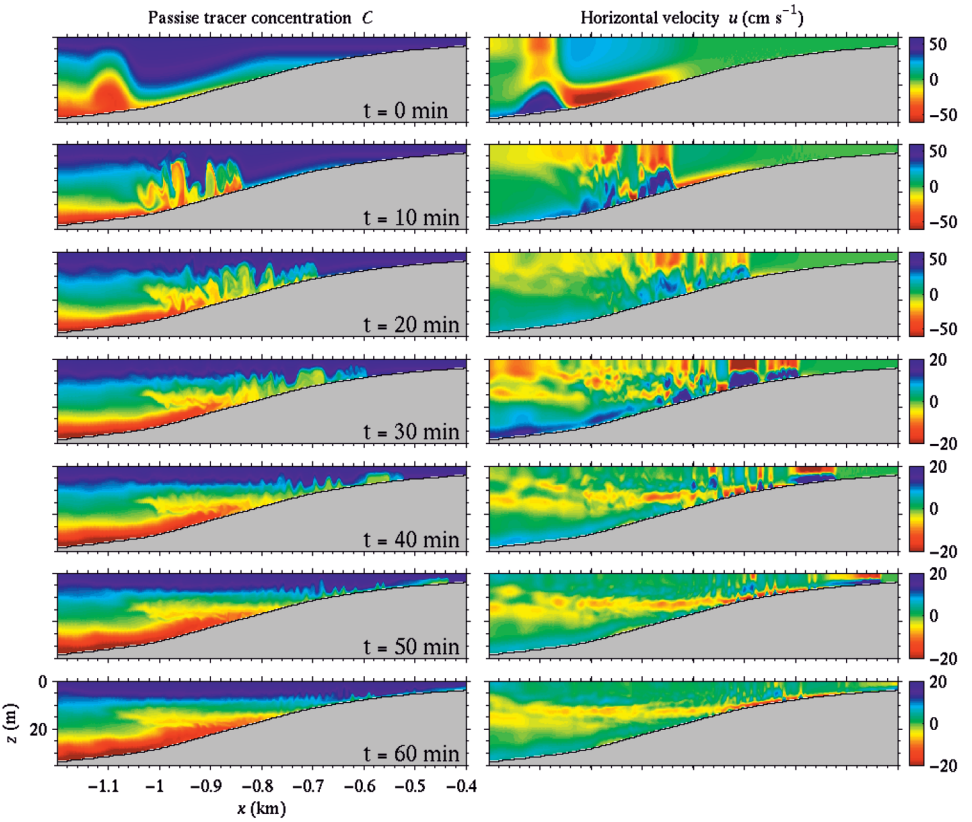

Figure 10. Simulated evolution of a passive scalar field C (left) and horizontal velocity u (right) upon impact of an internal solitary wave with the sloping boundary of Ile-aux-Lièvres. Note that the velocity scale changes between the third and fourth panels.

with the scaling factor z_0 arbitrarily set to 1 m. This tracer was then allowed to advect and diffuse as a passive scalar.

Figure 10 (left panels) shows the distribution of C during breaking and run-up, at times corresponding to those of Figure 9. In the early stage of the breaking/run-up process (around $t = 10$ min), an offshore propagating and undulating feature emerges at around 20 m depth. This feature later develops into a well-defined 10 m thick intermediate layer. By $t = 60$ min this layer has spread offshore by approximately 300 m. We note that this intermediate layer, located just below the pycnocline, is not clearly seen in the density field (Fig. 9).

The development of this intermediate layer is reminiscent of the Helfrich (1992) laboratory observations of a patch of dye spreading as an intermediate intrusive layer during wave breaking and swashing; compare his Figure 5 with our Figure 10. The numerical simulations presented here also reveal that this intermediate layer is mostly

composed of near-bottom water initially found below ~30 m in the undisturbed state. This suggests that ISW breaking on Ile-aux-Lièvres may provide a mechanism for generating intermediate nepheloid layers if the wave-induced bottom shear stress is sufficient to suspend sediments. This hypothesis remains to be tested in the field.

The signature of this intermediate layer is also seen in the horizontal velocity (Fig. 10, right panels). For $t \geq 40$ min, i.e. at times when most of the transient features and boluses have evolved up-slope past the wave breaking region, this intermediate layer is characterized with an offshore velocity of roughly 0.1 m s^{-1}, centered around the 12 m isobath. The velocity of this layer is consistent with the previous remark that the layer had spread 300 m offshore in approximately 50 min.

5. Discussion and conclusion

Our goal was to follow up on the work of Bourgault and Kelley (2003), in which remote sensing of surface roughness was used to identify ISW packets within the St. Lawrence Estuary. The new work involved sampling within the water column, with an emphasis on the region inshore of the wave-breaking zone. It also involved the use of a numerical model to simulate regions and scales unaddressed by the field measurements.

The new field measurements and numerical simulations lend support to the hypothesis of Bourgault and Kelley (2003) that internal waves impinge upon Ile-aux-Lièvres. Whether these ISWs are causing the mixing rates predicted by Bourgault and Kelley (2003) remains to be settled by *in situ* field turbulence measurements.

The simulations also suggest that ISW collision with the sloping topography of Ile-aux-Lièvres generates boluses of turbulent water that move onshore from the breaking zone. The modeled boluses are reminiscent of those observed in the laboratory, and the similarity of each to our time-series measurements near Ile-aux-Lièvres suggests that bolus generation indeed occurs at this site. Since this transported water comes from below the pycnocline of the estuary interior, this flux could have biological consequences to the ecosystem near Ile-aux-Lièvres.

Another result of ISW collision is suggested by the simulations. This is the generation of an intrusive layer extending from the mixing zone back into the estuary interior. Potentially, measurement of this return flow would provide a means of measuring the net effect of mixing at a site, solving the vexing issue of measuring sporadic and spatially-limited mixing events. In the present case, however, the sampling protocol was not able to provide details of the intrusion phenomenon. Our conclusions rely instead on numerical simulations and their similarity to observations in the laboratory (Helfrich, 1992; McPhee-Shaw and Kunze, 2002). This intrusive layer will not be easy to observe in density sampling (compare Figs. 10 and 9), but high-resolution velocity measurements may resolve its predicted 0.1 m s^{-1} velocity and 10 m vertical scale.

Guided by our results, it may be possible to design a field program capable of measuring not just the rate of mixing within internal wave breaking zones, but also the fluid transports associated with the related effects of boluses and intrusive layers. Such measurements

would move us closer to the goal of parameterizing mixing and other residual effects induced by internal waves that are prominent in many coastal zones.

Acknowledgments. This work was supported by the Department of Fisheries and Oceans of Canada (Galbraith), the Natural Sciences and Engineering Research Council of Canada (Kelley), the Canadian Foundation for Climate and Atmospheric Sciences (Kelley) and by the Fonds Québécois de la Recherche sur la Nature et Les Technologies (Bourgault).

REFERENCES

Bédard, J., A. Nadeau, J.-P. L. Savard and M. C. S. Kingsley. 1997. La passe de l'Ile aux Lièvres: importance stratégique pour la faune marine de l'estuaire, Tech. Rep. 283, Environment Canada, Canadian Wildlife Service.

Bourgault, D. and D. E. Kelley. 2003. Wave-induced boundary mixing in a partially mixed estuary. J. Mar. Res., *61,* 553–576.

—— 2004. A laterally averaged nonhydrostatic ocean model. J. Atmos. Oceanic Technol., *21,* 1910–1924.

Bourgault, D., F. J. Saucier and C. A. Lin. 2001. Shear instability in the St. Lawrence Estuary, Canada: A comparison of fine-scale observations and estuarine circulation model results. J. Geophys. Res., *106,* 9393–9409.

Government of Canada. 1997. Atlas of Tidal Currents from Cap de Bon-Désir to Trois-Rivières, Canadian Hydrographic Service, Fisheries and Oceans Canada, Ottawa.

Helfrich, K. R. 1992. Internal solitary wave breaking and run-up on a uniform slope. J. Fluid Mech., *243,* 133–154.

McPhee-Shaw, E. E. and E. Kunze. 2002. Boundary-layer intrusions from a sloping bottom: A mechanism for generating intermediate nepheloid layers. J. Geophys. Res., *107,* 3050, doi:10.1029/2001JC000801.

Michallet, H. and G. N. Ivey. 1999. Experiments on mixing due to internal solitary waves breaking on uniform slopes. J. Geophys. Res., *104*(C6), 13467–13477.

Pelletier, E. and J. Lebel. 1979. Hydrochemistry of dissolved inorganic carbon in the St. Lawrence Estuary (Canada). Estuar. Coast. Shelf Sci., *9,* 785–795.

Saucier, F. J. and J. Chassé. 2000. Tidal circulation and buoyancy effects in the St. Lawrence Estuary. Atmosph. Ocean, *38,* 1–52.

Vlasenko, V. and K. Hutter. 2002. Numerical experiments on the breaking of solitary internal waves over a slope-shelf topography. J. Phys. Oceanogr., *32,* 1779–1793.

Received: *28 June, 2004;* revised: *19 May, 2005.*